Dolomitization of the Silurian Niur Formation, Tabas Block, east central Iran: Fluid flow and dolomite evolution

Article *in* Marine and Petroleum Geology · July 2016

DOI: 10.1016/j.marpetgeo.2016.07.023

CITATIONS
3

READS
427

5 authors, including:

A. Mahboubi
Ferdowsi University Of Mashhad
133 PUBLICATIONS **863** CITATIONS
SEE PROFILE

Zohreh Nowrouzi
Hakim Sabzevari University
4 PUBLICATIONS **31** CITATIONS
SEE PROFILE

Ihsan Al-Aasm
University of Windsor
160 PUBLICATIONS **3,291** CITATIONS
SEE PROFILE

R. Moussavi-Harami
Ferdowsi University Of Mashhad
154 PUBLICATIONS **1,177** CITATIONS
SEE PROFILE

Marine and Petroleum Geology 77 (2016) 791–805

Contents lists available at ScienceDirect

Marine and Petroleum Geology

journal homepage: www.elsevier.com/locate/marpetgeo

Research paper

Dolomitization of the Silurian Niur Formation, Tabas block, east central Iran: Fluid flow and dolomite evolution

A. Mahboubi [a, *], Z. Nowrouzi [b], I.S. Al-Aasm [c], R. Moussavi-Harami [a], M.H. Mahmudy-Gharaei [a]

[a] Department of Geology, Faculty of Science, Ferdowsi University of Mashhad, Mashhad, Iran
[b] Faculty of Science, Hakim Sabzevari University, Sabzevar, Iran
[c] Department of Earth and Environmental Sciences, University of Windsor, Windsor, Canada

ARTICLE INFO

Article history:
Received 7 March 2016
Received in revised form
5 July 2016
Accepted 22 July 2016
Available online 25 July 2016

Keywords:
Hydrothermal dolomitization
Fluid evolution
Silurian
Iran

ABSTRACT

The Silurian Niur carbonates at Dahaneh-Kalut and Ozbak-Kuh sections (Tabas block, eastern Central Iran) have been pervasively dolomitized. Four types of dolomite, consisting of replacive dolomite (Rd1–Rd3) and saddle dolomite cements (Cd), were discriminated by texture, cathodoluminscence petrography and geochemical analyses. Rd1 dolomite occurred as a very fine (10–25 μm), planar-e to planar-s dolomite that replaced marine limestones. Rd2 dolomite is a planar-s to planar-e, medium crystalline dolomite (100–400 μm). Rd3 dolomite is a very coarse (400 μm–2 mm), non-planar crystalline dolomite with sweeping extinction, and Cd dolomite occurred as voids- and fractures-filling saddle dolomite (5–10 mm) with strong sweeping extinction. Field and petrographic observations demonstrated that Rd3 and Cd occur only at the Dahaneh-Kalut section and are related to mafic volcanic rocks and fractures at the base of the Niur Formation. The $\delta^{18}O$ (−8.45 to −6.06‰ VPDB) and $\delta^{13}C$ (−0.01 to 0.99‰ VPDB) values suggest that Rd1 dolomite was precipitated at the early stage of dolomitization from Silurian seawater, whereas Rd2 dolomite formed from similar fluids at higher temperatures upon burial. The $\delta^{18}O$ (−13.80 to −9.47‰) and $\delta^{13}C$ (−1.66 to 0.76‰) values and fluid inclusion data (T_h: 122 to 175 °C, salinity: 18.68 to 24 wt% NaCl eq.) revealed that Rd3 and Cd were precipitated from hot, saline fluids with a magmatic origin. The Mn, Fe, Na and Sr concentrations of Rd3 and Cd, suggest that the responsible dolomitizing fluids were more enriched with respect to these elements and had a different origin relative to the Rd1 and Rd2 dolomitizing fluids. These results revealed that the late Ordovician to early Silurian passive rifting phase generated a local thermal gradient that increased heat flow and thermal convection of diagenetic fluids that led to the precipitation of Rd3 and Cd as pervasive hydrothermal dolomite. The network of fractures and faults that formed during the rifting phase provided open conduits for hydrothermal fluids. These results emphasize the importance of both tectonic setting and thermal conditions in the generation and circulation of dolomitizing fluids as well as in massive dolomitization.

1. Introduction

The formation of massive dolostones in the geologic record is still poorly understood phenomenon (Fu et al., 2006; Lavoie et al., 2010; Jacquemyn et al., 2014). Host rock permeability, hydraulic gradient, fluid chemistry, kinetic factors and the time of formation are major parameters controlling dolomitization (Machel and Lonnee, 2002; Nader et al., 2004; Al-Aasm et al., 2009; Lavoie and Chi, 2010; Azomani et al., 2013). Also, dolostones host large volumes of oil and gas as well as MVT and SEDEX base metal deposits. The Silurian Niur Formation is pervasively dolomitized and is found in most parts of Tabas Block in Central Iran. Despite several paleontological studies on the Niur Formation (e.g., Flügel, 1962; Flügel and Saleh, 1970; Hairapetian et al., 2008, 2011), there has been no specific study on the origin of its dolostones and hence the mechanism of dolomitization remains unknown. This study is the first attempt to determine the origin of the pervasive dolomitization of the Niur Formation in the eastern part of Central Iran. In this

* Corresponding author.
E-mail address: mahboubi@um.ac.ir (A. Mahboubi).

http://dx.doi.org/10.1016/j.marpetgeo.2016.07.023
0264-8172/

study, we report field, petrographic investigations, geochemical analyses and microthermometric results of dolomite samples from two Silurian stratigraphic sections, as well as from a few dolostone samples from the Ordovician Shirgesht Formation. A model is developed to account for the massive dolomitization that is found at the Ozbak-Kuh and Dahaneh-Kalut sections. Dolomitization in the Niur Formation is a good example of dolomite formation in a rifting tectonic setting showing the control of magmatic activities on the dolomitization process.

2. Geological and tectonic setting

The Iranian plate, along with a number of smaller tectonic zones (Central Iran, Alborz and Sanandaj- Sirjan) of probable Gondwanan or peri- Gondwanan affinity, was part of the larger Cimmerian continent during the evolution of the Paleo-Tethys and Neo-Tethys oceans (Sengör, 1987). The study area (Fig. 1) is located on the eastern side of central Iran and it is surrounded by fold-and-thrust belts within the Alpine–Himalayan orogenic system of western Asia (Nadimi, 2007). Central Iran is an area of continuous continental deformation because of the ongoing convergence between the Arabian (Gondwana) and Turan plates (Nadimi, 2007). These plates are separated by the eastern Tabas and western Yazd tectonic blocks. The Tabas block is defined by the Nayband fault to the east and the Kalmard-Kuhbanan fault to the west (Alavi, 1996). The edges and interior of the Tabas structural domain are cut by several faults that extend to the basement. These N-S straddling faults have been linked to Katangan (late Precambrian) tectonic activity which affected most of the Tabas block (Aghanabati, 2004). Thus the sedimentary facies and their distribution in the Tabas block are related to block faulting (e.g., Lasemi, 2001). The Niur Formation, which was deposited during the opening and Silurian evolution of the Paleo-Tethys Ocean (Berberian and King, 1981), was affected by NE-SW faults that are linked to this rifting event (Aghanabati, 2004). The type section of the Niur Formation in the Gusheh-Kamar Mountains is located at Ozabak-Kuh and correlative reference section in the Derenjal Mountains. Both of these sections are located on the eastern side of the Tabas Block (Fig. 1).

In the reference section, there are sedimentary exposures from Cambrian (Barut, Zagun and Lalun formations) to Devonian (Bahram Formation) time (Fig. 2). The Cambrian formations are composed of sandstone and shale whereas the Ordovician (Shirgesht) formations are composed of shale and marl (Aghanabati, 2004). The type section is dominated by massive dolostone and the middle parts of these successions are composed of silty and sandy dolomitic limestones. Dolomitic coralline limestones are dominant in the upper parts of this succession. The Reference section is mainly composed of shallow bioclastic limestones, white sandstone and shale. The lower parts of this section consist of mafic submarine volcanic rocks, which are attributed to Upper Ordovician-Lower Silurian intracontinental rift event (Aghanabati, 2004) that led to separation of the Turan from the Iran plate and Paleo-Tethys formation. In this section, the bioclastic limestones are very rich in dolomitized corals and brachiopods and these carbonates are completely dolomitized in the vicinity of mafic volcanic rocks in the lower parts of the reference section. Chaotic and crackle clast-supported breccias with angular clasts occur also in the dolomitic lithofacies. Coralline limestones in the upper part of the Niur Formation are partially dolomitized and mainly related to shoal facies. White sandstones form a conspicuous and mappable member in the middle part of this formation. Planar and herringbone cross stratifications are very common in these sandstones. These sandstones are mainly cemented by silica and dolomite. The basal contact of the Niur Formation at type section with the uppermost Cambrian to Middle Ordovician Shirgesht Formation is faulted, whereas at Dahaneh-Kalut section this contact is characterized by the presence of mafic volcanic rocks (Fig. 3). The upper boundary of this Formation is conformable with the Devonian Padeha (mixed silisiclastic, dolomitic and evaporitic rocks) Formation (Ruttner et al., 1968).

3. Materials and methods

More than 350 samples were collected from outcrops of the Niur Formation (Fig. 3) at the Ozbak-kuh type and Dahaneh-Kalut reference sections in addition to 10 samples from the Ordovician Shirgesht Formation. Petrographic analyses were performed on selected 300 thin sections that were stained with mixture of alizarine red and potassium ferricyanide solution (Dickson, 1965). Dolomite types were differentiated on the basis of the classifications of Gregg and Sibley (1984), Sibley and Gregg (1987), Mazzullo (1992) and Chen et al. (2004). In addition, 20 polished thin sections were examined under a cathodoluminescence microscope using a Technosyn Cold CL (Model 8200 MK3) at 12 kV and 195 μA. To investigate the dolomite texture and porosity, scanning electron microscopy (SEM) analyses were conducted on six representative gold-coated samples using a 145OVP model SEM LEO at the central lab of the Ferdowsi University of Mashhad.

Forty dolostone samples from the Niur Formation and 4 dolostone samples from the Shirgesht Formation were micro-drilled for their dolomite and calcite types and analyzed for their $\delta\ ^{13}C$ and $\delta\ ^{18}O$ ratios. Because of our samples were micro-drilled then the analyzed samples aren't mixtures of the different dolomite phases and only single phases were analyzed. Samples of about 30–80 μg of pure carbonates were loaded into stainless steel boats. The samples were then heated under vacuum at 200 °C for one hour to release any volatile organic compounds. Both samples and standards were transferred individually to glass vials and reacted for 4 min under vacuum using 3 drops of 100% phosphoric acid at 75 °C at the Keck Paleoenvironmental and Environmental Stable Isotope Laboratory (KPESIL) of the University of Kansas, USA. Analyses were carried out using a Kiel Carbonate Device III connected to the inlet of a Thermo Finnigan MAT253 isotope-ratio mass spectrometer. All isotope data are reported relative to the Vienna Pee Dee Belemnite (VPDB) standard with analytical precision of better than ± 0.1‰ for both the $\delta\ ^{13}C$ and $\delta\ ^{18}O$ ratios. Twenty-five samples were also analyzed using an ICP-OES Perkin Elmer Optima 5300DV in the geochemistry laboratory of the University of Kansas to determine their Ca, Mg, Sr, Na, Mn and Fe contents with 10% analytical precision.

Five doubly-polished wafers of dolomite were prepared for fluid inclusion microthermometry, which were done at the Iranian Mineral Processing Research Center (IMPRC). Both homogenization (T_h) and final ice melting temperatures (T_{mice}) were measured. The former is the inclusion's minimum entrapment temperature (i.e. the temperature of mineral precipitation) (Goldstein and Reynolds, 1994). The latter, is the temperature at which the last ice melts in an aqueous fluid inclusion, which reflects the trapped diagenetic fluid's salinity (Goldstein and Reynolds, 1994). The measured T_{mice} value were utilized to calculate the wt.% NaCl eq. using the relationship of Hall et al. (1988) and Bodnar (2003). Carbonate rocks are soft and vulnerable to overheating. Therefore, doubly polished wafers were prepared using resin and hardener and the thin-section preparation method of Roedder (1984) so that the wafers would not be affected by thermal stresses during preparation. These samples were selected from the first dolomite units in the Dahaneh-Kalut section that were formed in the vicinity of submarine volcanic rocks. To determine if the inclusions were primary or secondary or pseudosecondary, detailed petrographic studies were carried out under a Zeiss microscope (Goldstein and Reynolds,

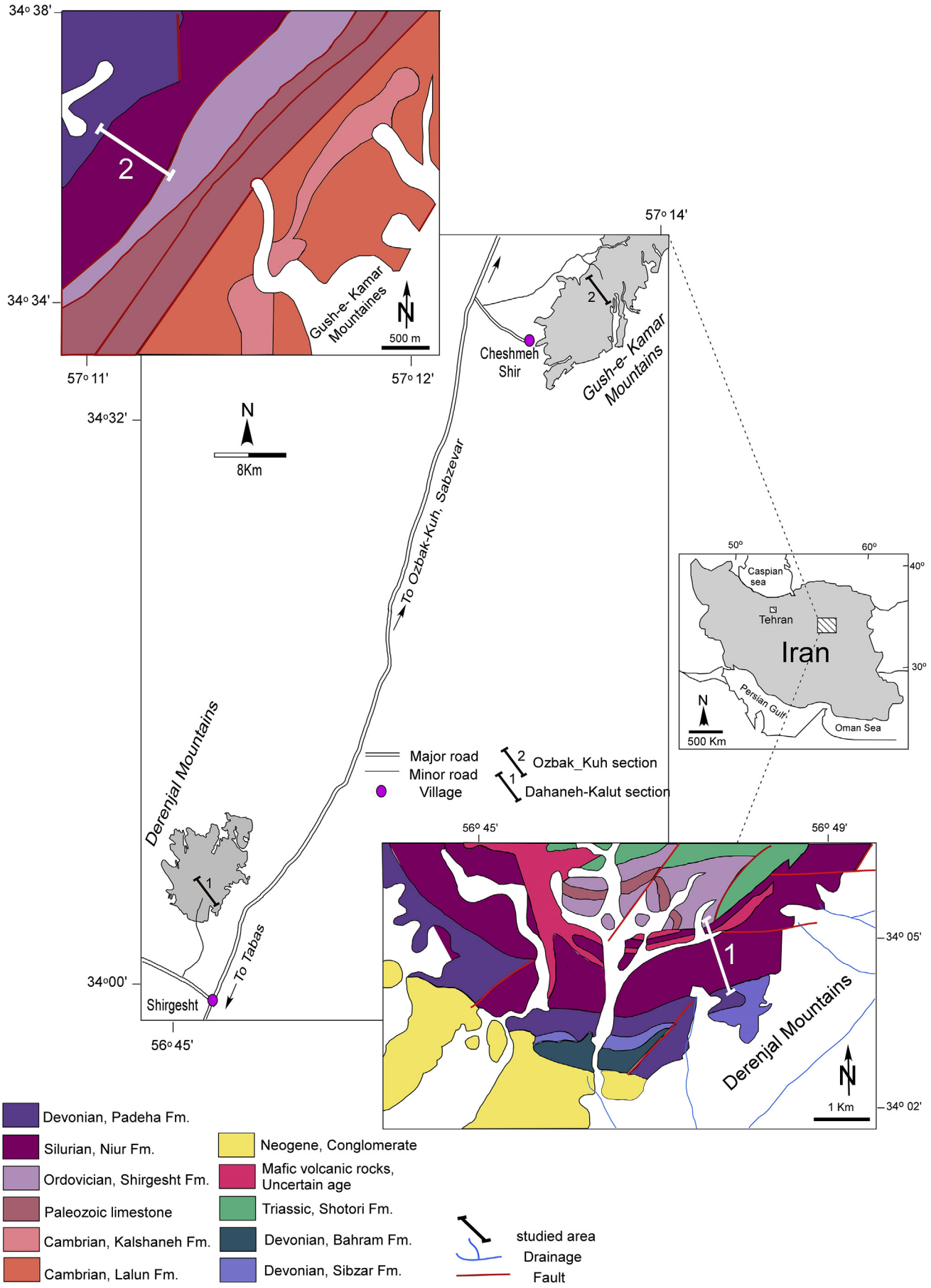

Fig. 1. Location and geological maps of the measured sections at: 1) Derenjal Mountains (Dahaneh-Kalut section) and 2) Gusheh-Kamar Mountains (Ozbak-Kuh section) (modified from Ruttner et al., 1968).

1994). Also, in the determination of primary fluid inclusions, the arrangement of the inclusions, the crystal boundaries and other mineralogic properties were examined (Roedder, 1984). Hence, fluid inclusion microthermometric measurements were carried out on isolated primary, two-phase liquid-vapor fluid inclusion assemblages using a Linkam THMS 600 heating-freezing stage at the Iranian Mineral Research Center's lab. Calibration with a precision of ±0.6 C at +414 °C and ±0.2 at −94.3 °C was measured using cesium nitrate and n-Hexane fluid inclusion standards.

4. Results

4.1. Field observations

The Niur Formation is composed of carbonate and siliciclastic rocks that were precipitated in high energy, shallow marine (Nowrouzi et al., 2014) to low energy, open marine and basinal environments during Silurian time. Dolomitization of Nuir carbonate rocks is a very common diagenetic process in the both studied stratigraphic sections. In the lower parts of the Dahaneh-Kalut and Ozbak-Kuh sections, dolomitization is pervasive whereas in the upper parts it changes to partial dolomitization. In the Dahaneh-Kalut section, the dolostone facies consist of massive yellowish dolostone breccias (Fig. 4a) and grey to yellow, stratiform, non-brecciated dolostone (Fig. 4b), whereas only non-brecciated dolostone has been observed in the Ozbak-Kuh section. Both replacive and fracture-filling dolomite types are more common in the Dahaneh-Kalut section whereas only replacive dolomite is found in the Ozbak-Kuh section. In the vicinity of mafic volcanic rocks at the base of the Dahaneh-Kalut section, dolomite cement filled the intergranular spaces of fractured and brecciated dolostones, whereas larger crystal sizes of replacive dolomite formed in the brecciated or non-brecciated dolostones. The mafic volcanic rocks are black to very dark green with pillow structures (Fig. 4b and c) and contain fractures that are related to the Ordovician - Devonian rifting phase in the Central Iran Block and to the opening of Paleo-Tethys Ocean in the Late Ordovician-Early Silurian. Most fractures usually have E-W or NE-SW trends although in some cases there is also a network of fractures with different trends that are related to a Precambrian tectonic event (Aghanabati, 2004) (Fig. 4d). Both sets of fractures (E-W and NE-SW) are usually filled with large, white and yellow crystals of saddle dolomite. Brecciation of the dolostones led to the formation of mosaic and crackle breccias in the Dahaneh-Kalut succession. The dolostone breccias are massive, irregular and clast supported, and they form limited and unextended macropores at the base parts of the Dahaneh-Kalut section. The clasts are yellow to grey in color, medium to large (long axis: 2–20 cm) in size, angular to semi-angular in shape, and are also composed of large crystals of replacive dolomite (Rd3). The intergranular spaces of these breccias are filled by large, yellow to red crystals of saddle dolomite (Cd) (Fig. 4a). Laterally, the brecciated dolostone passes into stratiform, non-brecciated dolostone.

4.2. Petrography, mineralogy and paragenesis

Calcite, dolomite and sulphides are the main diagenetic mineral phases recorded in the studied rocks (Nowrouzi, 2015). Limestone is mainly packstone and grainstone with skeletal grains that contain brachiopods, echinoderms, bryozoans and corals. Petrographic evidence, such as concave-convex contacts, deformed grains and stylolitization, demonstrate that chemical and physical compaction and fracturing are extensive diagenetic features.

4.2.1. Calcite cements

Three types of calcite cement were identified in fossils, void spaces and fractures. They are: 1) syntaxial overgrowth that surrounded echinoderms (C1, Figs. 5a) and 2) non-ferroan (100–200 μm) calcite cement (C2, Figs. 5b) and 3) ferroan coarse (300 μm to 2 mm) blocky calcite that mainly filled fractures (C3, Fig. 5a and b). In most samples, the C1 and C2 were mainly replaced by dolomite, whereas the C3 type formed after saddle dolomite.

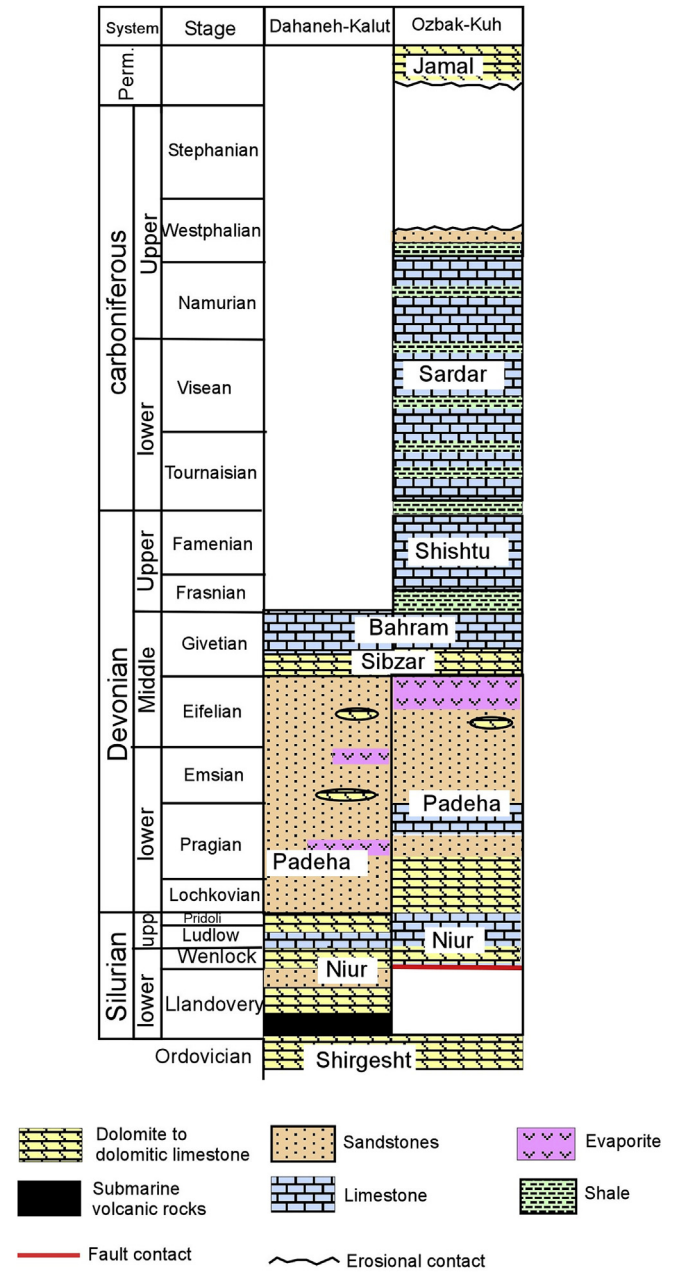

Fig. 2. Stratigraphy framework of Ordovician to Permian sediments of Dahaneh-Kalut and Ozbak-kuh sections.

4.2.2. Dolomite

Dolomitization is represented by both replacement and cement precipitation in the Dahaneh Kalut section, but it occurs as only as replacive dolomite in the Ozbak Kuh section.

4.2.3. Replacive dolomite types

4.2.3.1. Fine grained replacement dolomite Rd1. Rd1 dolomite has been found mainly in the upper part of the Ozbak-Kuh limestones

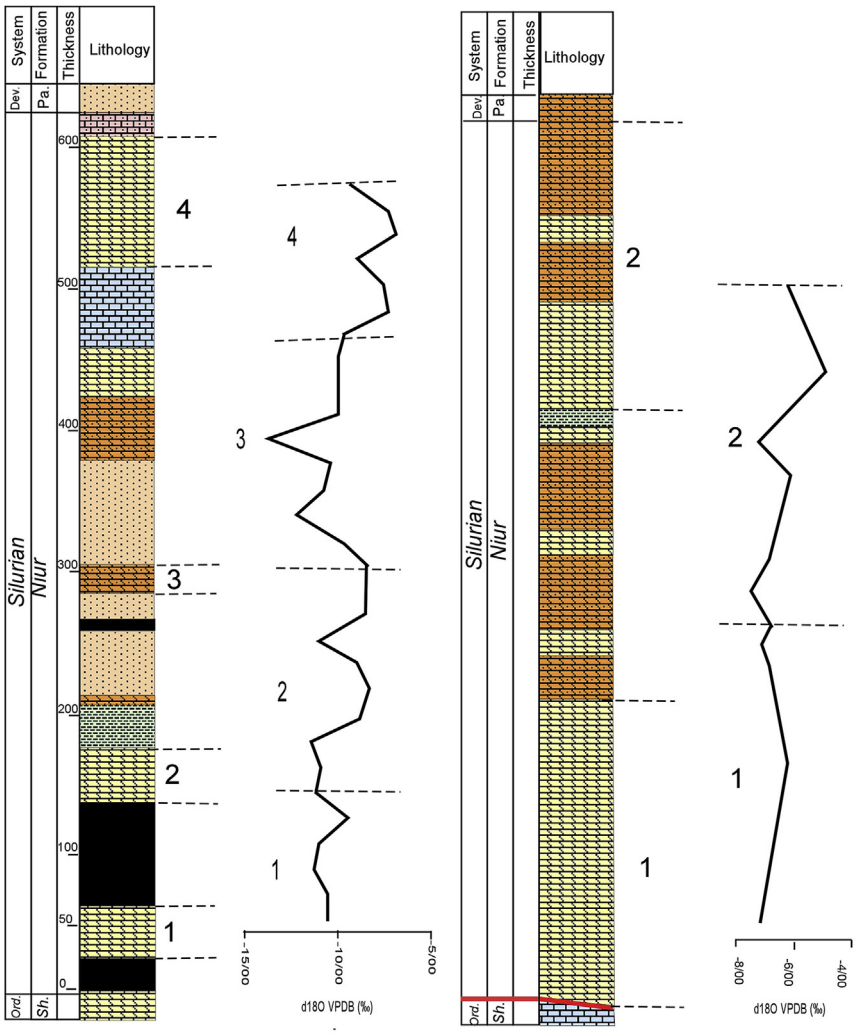

Fig. 3. Lithostratigraphic columns of the Niur Formation at the Dahaneh-Kalut (Left) and Ozbak-Kuh (Right) sections. This figure also illustrated the $\delta^{18}O$ of this Formation in two sections.

and the middle and upper parts of the Dahaneh-Kalut section. The dolomite crystals replaced skeletal grains such as corals, bryozoans and echinoderms and they are not related to post-depositional fractures. SEM and other petrographic observations show that the RD1 dolomite occurs as 10–25 μm, euhedral to planar-s crystals (Figs. 6a and 5b). Intercrystalline pore spaces and evidence of recrystallization, such as the existence of small crystals in the vicinity of larger crystals occur also in this type of dolomite (Fig. 6b). Rd1 dolomite has a dark to dull red mottled luminescence (CL) under cold cathodoluminoscope and it is non-ferroan. The Rd1 dolomite is more frequent in the upper part of the Dahaneh-Kalut section and forms about 20% of the overall volume of dolostones.

4.2.3.2. Medium grained replacement dolomite Rd2. Volumetrically, Rd2 dolomite constitutes about 60% of the dolostone present at Ozbak-Kuh and 40% at Dahaneh-Kalut. This dolomite occurs as 100–400 μm, euhedral to subhedral planar-s crystals. Less frequent planar-e crystals are polymodal with cloudy centers and clear rims, and they mostly replace lime mudstone. The planar-e crystals progressively change into planar-s crystals. Planar-s crystals are more abundant and replaced all grains as well as lime mud and calcite cements. In samples that are replaced by pervasive and destructive planar-s dolomite, precursor bioclasts and limestones are not identified and echinoderms are the only recognizable bioclasts (Fig. 6c). Rd2 dolomite has dark mottled CL.

4.2.3.3. Replacement saddle dolomite Rd3. The Rd3 is pervasive, fabric-destructive and fracture related saddle dolomite. It is observed near the basal submarine volcanic rocks in the Dahaneh-Kalut section. This dolomite type is also observed as patches in the upper parts of the Dahaneh-Kalut limestone. The crystals are non-planar and about 400 μm to 2 mm in size. Crystals show sweeping extinction (Fig. 6d) and they exhibit dull red to non CL. Rd3 dolomite usually replaced fractured carbonate rocks. Volumetrically, the Rd3 dolomite represents about 20% of the total amount of dolostone in the Dahaneh-Kalut section. This dolomite, which is usually cut by stylolites, was never observed in the Ozbak-Kuh section.

4.2.3.4. Saddle dolomite cement (Cd). Most of the remaining open spaces, including fractures and vugs, are filled with saddle dolomite (Cd) in the Dahaqneh-Kalut section (Figs. 6e and 7a). Volumetrically, this type of dolomite is not very abundant. It constitutes about 10% of the Dahaneh-Kalut section and is rare in Ozbak-Kuh section. The Cd dolomite is the most abundant cement between the clasts of replacive dolomite (Rd3) and breccia (Fig. 7b–d). This dolomite is

Fig. 4. Field photos of: a) yellowish, clast supported, dolostone breccias with angular to semi-angular clasts. Clasts are composed of replacive dolomite and open space filled by yellow to red large crystals of saddle dolomite; b) Non-bracciated massive dolomite (do) that formed at the vicinity of volcanic rock (vol) at the base of Dahaneh-Kalut section; c) Black to dark grey submarine volcanic rocks at the base of Dahaneh-Kalut section with pillow lava structures; and d) Network of fractures with NE-SW dominant trends. These fractures filled with white saddle dolomite crystals. (For interpretation of the references to colour in this figure legend, the reader is referred to the web version of this article.)

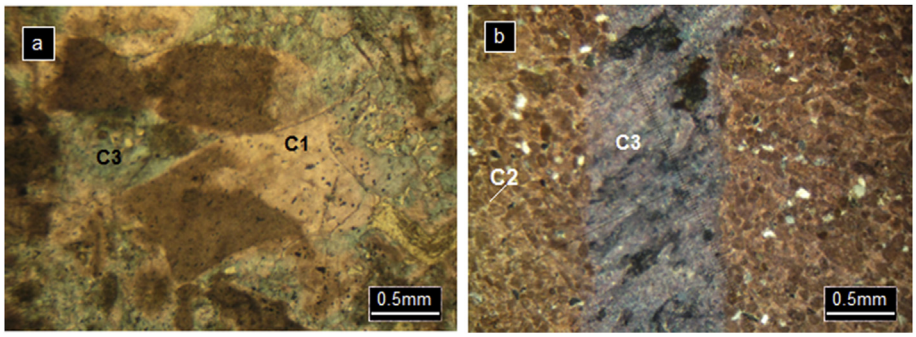

Fig. 5. Photomicrographs of cement types in the Niur Formation. a) Stained thin section of bioclastic grainstone facies, with non-ferroan syn-taxial calcite cement (C1) and ferroan blocky cement (C3); and b) Stained thin section of the peloidal grainstone facies, with non-ferroan calcite cement (C2) that filled porosity space and fracture filling ferroan blocky cement (C3).

fracture and vug filling (Fig. 7a), and mostly formed in the vicinity of submarine volcanic rocks. The 5–10 mm crystals show a strong sweeping extinction. This dolomite exhibits general dull red CL but rarely CL zonation in some samples (Fig. 8). The CL-zoned crystals are mostly found in the upper part of the Dahaneh-Kalut section. Also the Cd dolomite crystals are usually cut by stylolites (Fig. 6e), and they show corroded and broken rims.

4.2.3.5. Sulfide minerals. Pyrite is the most common sulfide mineral to have precipitated after saddle dolomite (Fig. 6f). SEM and EDX analyses also demonstrated the existence of sphalerite and pyrite in the spaces between breccia clasts and these sulfides represent the last diagenetic phases in the paragenetic sequence (Fig. 9).

4.3. Geochemistry

4.3.1. Stable isotopes

Carbon and oxygen stable isotope data in the Ozbak-Kuh and Dahaneh-Kalut sections were bring in Table 1. Twelve samples from the Ozbak-Kuh section yielded $\delta^{18}O$ values of −4.70‰ to −7.66‰ VPDB (Rd1 = −6.06‰ to −6.37‰VPDB, Rd2 = −4.70‰ to −7.66‰ VPDB) and $\delta^{13}C$ values from 1.25‰ to −0.36‰ VPDB (Rd1 = 0.35‰ to 0.98‰VPDB, Rd2 = −0.36‰ to 1.25‰VPDB). A further thirty samples from the Dahaneh-Kalut section yielded $\delta^{18}O$ values of −6.99‰ to −13.80‰ (Rd1 = −6.99‰ to −8.45‰VPDB, Rd2 = −8.52‰ to −9.54‰VPDB, Rd3 = −9.47‰ to −11.21‰VPDB, Cd = −9.87‰ to −13.80‰VPDB) and $\delta^{13}C$ values from −1.05‰ to 1.30‰ VPDB (Rd1 = 0.99‰ to −0.01‰VPDB; Rd2 = 0.73‰ to −0.36‰VPDB; R3 = 1.30‰ to - 0.57‰VPDB; Cd = 1.30‰ to −1.66‰VPDB, respectively).

4.3.2. Major and trace elements

Table 1 summarizes the major and trace element concentrations of the different dolomite types in the Ozbak-Kuh and Dahaneh-Kalut sections. Rd3 (Ca: 52–58 mol %) and Cd (Ca: 55–58 mol %) dolomite types are calcium-rich and non-stoichiometric and have higher Sr concentrations (73–122 ppm and 72–120 ppm, respectively) than Rd1 and Rd2. Rd1 dolomite is more calcium-rich and has higher Sr concentrations than Rd2 at Ozbak-Kuh (Rd1, Ca: 53 mol%, Sr: 95 ppm, n = 1; Rd2, Ca: 50–52 mol%, Sr: 49–61 ppm n = 6) and Dahaneh-Kalut (Rd1, Ca: 53 and 54 mol% Sr: 74 and 73 ppm, n = 2, Rd2; Ca: 51–52 mol% Sr: 40–56 ppm, n = 2) sections. Although the Fe and Mn concentrations are enriched at Dahaneh-Kalut compared with Ozbak-Kuh, the Rd2 dolomite

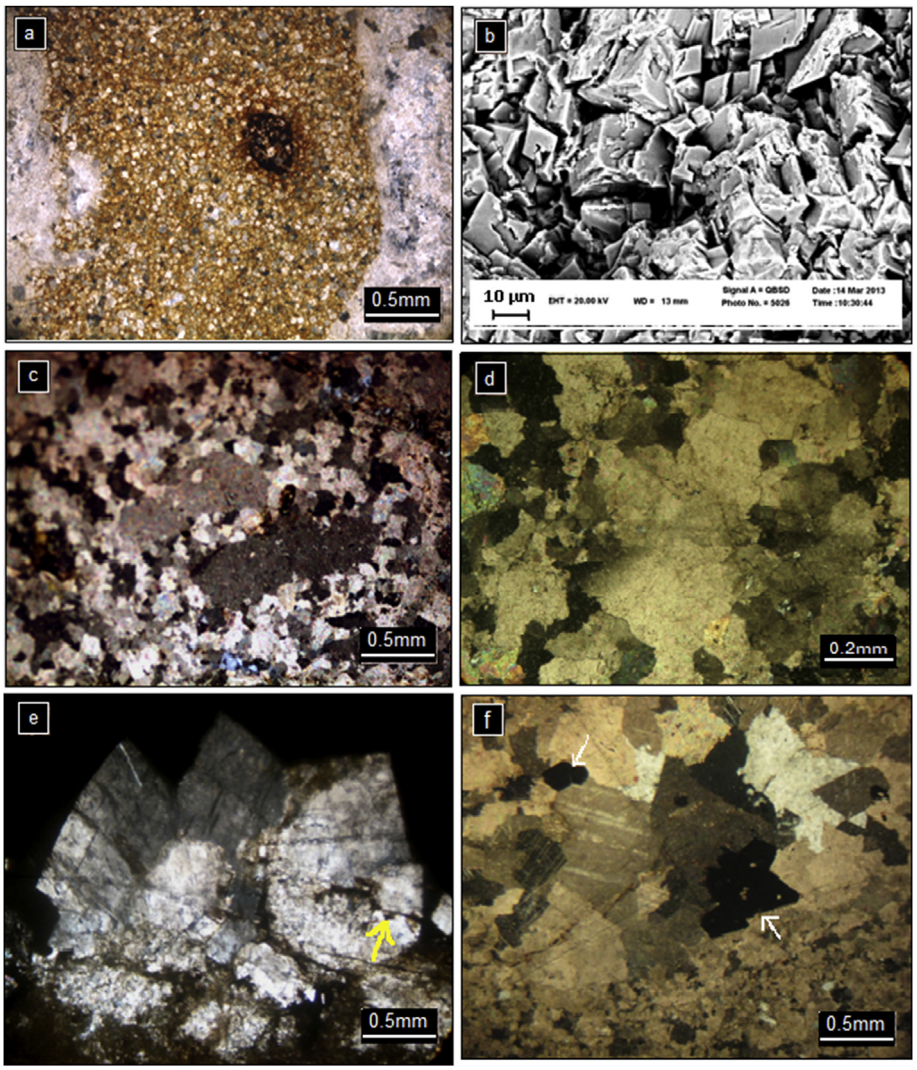

Fig. 6. a) Photomicrograph showing coralline limestone that is replaced by fine crystalline, planar-e Rd1 dolomite (XPL); b) SEM photomicrograph of fine planar-e to planar-s Rd1 dolomite; c) bioclastic limestone that is replaced by non-planar to planar-s Rd2 dolomite, echinoderms that are theonly recognizable bioclasts in this destructive and pervasive dolomite (XPL); d) non-planar, xenotopic-a, Rd3 dolomite with sweeping extinction (XPL); e) saddle like, Cd dolomite that has a lobate and corroded rim (XPL); and f) sulfide mineralization (arrow:pyrite) that formed after the saddle dolomite (XPL).

generally has similar concentrations in both sections (Fe: 3340–9974 ppm, Mn: 439–1123 ppm n = 8). The highest Fe and Mn concentrations belong to Rd3 (Fe: 10,702–21,990 ppm, Mn: 1550–5470 ppm) and Cd (Fe: 11,832–24,221 ppm, Mn: 1178–4702 ppm) in the Dahaneh-Kalut section. Na concentrations vary between 79 ppm for Rd2 dolomite at Ozbak-Kuh and 656 ppm for Rd3 at Dahaneh-Kalut.

4.4. Fluid inclusions

Microthermometric measurements were carried out on 31 isolated primary two-phase, liquid-vapor, isolated fluid inclusions (Fig. 10) in Rd3 (n = 11) and Cd (n = 20) dolomite types (Table 2). Due to the fact that Rd1 and Rd2 had too small crystals and no two phase fluid inclusions were found, microthermometric measurements were not possible for them. Fluid inclusions of Rd3 and Cd were very small and ranged from <3 μm for Rd3 and 3–6 μm for Cd, respectively with a liquid portion of ~75% and vapor bubbles occupying 25% of the inclusions. Whereas some all-liquid inclusions were found in Rd3, Cd dolomite entirely hosted two phase liquid-vapor fluid inclusions. Measurements were taken from the both parts of rim and core of the Rd3 and Cd crystals. The minimum temperature of mineral formation is given by the homogenization temperature (Th). Homogenization temperatures (T_h) in the Rd3 and Cd dolomite types ranged from 122° to 163 °C and from 130° to 175 °C, respectively (Fig. 11). Due to the small size of the inclusions the last ice melting temperature (T_{mice}) and salinity was not measured for RD3 dolomite but for the Cd dolomite the T_{mice} ranged from −15 °C to −27 °C, which corresponds to salinities of 17–24 wt% NaCl equivalent (Bodnar, 2003) (Fig. 12).

5. Discussion

5.1. Constraints from field relationships and petrography

Rock texture can provide a useful indication of the thermal conditions under which dolomite types are formed. The larger crystal size of Rd2 than Rd1 dolomite types suggests that Rd2 was formed at a deeper setting relative to that of Rd1. Fluid inclusions studies revealed that Rd1 is dominated by all-liquid phase, which

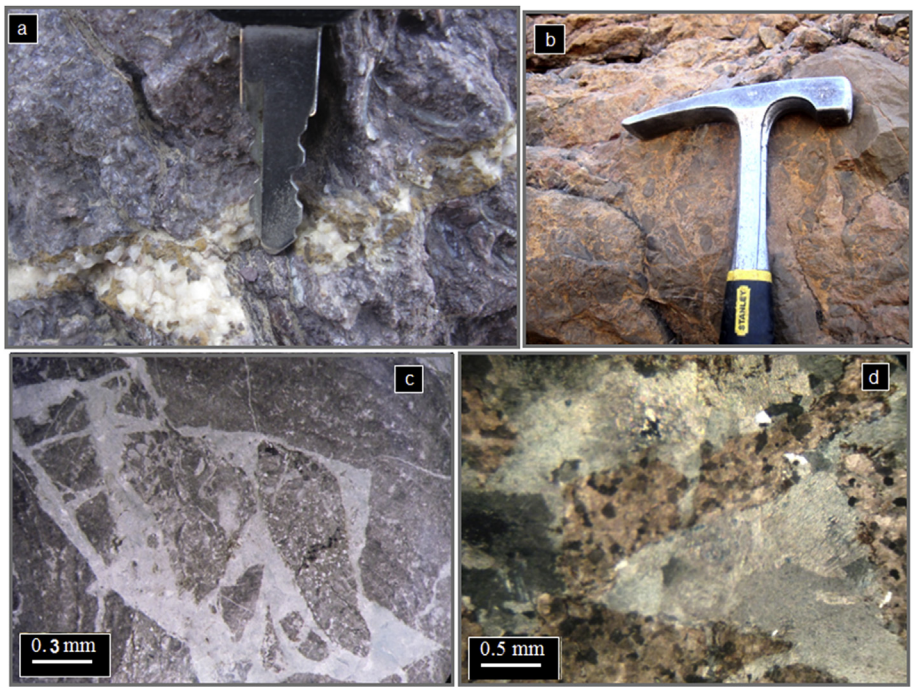

Fig. 7. a) Fracture-related Rd3 and Cd dolomite; b) field photo of crackle breccia; c) photomicrograph of crackle to mosaic breccia that is filled with Cd dolomite (PPL); and d) mosaic breccias with Rd3 clasts within Cd dolomite cement (XPL).

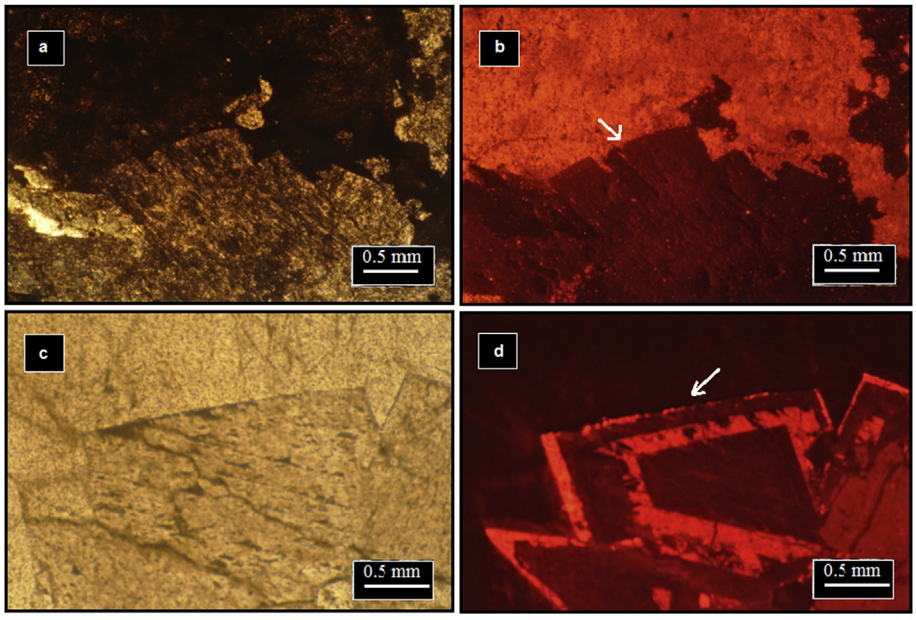

Fig. 8. a & b) PPL and CL pair of photographs of Cd dolomite (arrow); c & d) PPL and CL pair of photographs that show CL zonation in Cd dolomite (arrow).

suggest that it was probably formed <50 °C or at the most around 60 °C. Lack of evaporites suggests that this dolomite was not formed from evaporative brines such as in sabkha environment (Olanipekun et al., 2014). Field observations revealed that Rd3 and Cd are fracture-related and formed in the lower parts of Dahaneh-Kalut in the vicinity of mafic volcanic rocks. Large crystal size, curved crystal faces and undulatory extinction demonstrated that Rd3 and Cd formed in a high temperature and pressure realm of deep burial setting (Gregg and Sibley, 1984; Al-Aasm, 2000; Warren, 2000; Azmy et al., 2009 (BCPG); Azomani et al., 2013; Olanipekun et al., 2014; Hou et al., 2016). Dolostones at Dahaneh-Kalut have been subjected to some brecciation. Breccia body shapes are vein-like and irregular to spherical similar to what that Davies and Smith (2006) described. Clasts of breccia are represented by Rd3 crystal types and open spaces filled with Cd dolomite (Fig. 7). This brecciation can be related to hydrothermal fluid effects (e.g. Davies and Smith, 2006), perhaps in close proximity to fault zones.

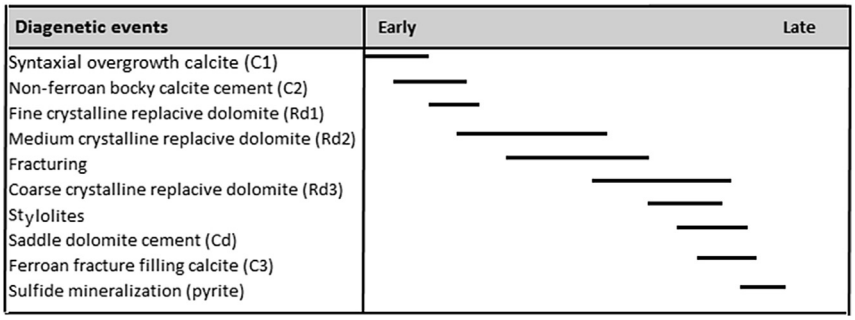

Fig. 9. Paragenetic sequence for the Niur Formation in Tabas block.

Table 1
Statistic summary of geochemical composition ($CaCO_3$, $MgCO_3$, Mn, Fe, Sr, $\delta^{13}C$ and $\delta^{18}O$) of the Niur Formation dolomite at Dahaneh-Kalut and Ozbak-Kuh sections.

Dolomite types		Ca (mol%)	Mg (mol%)	Na (ppm)	Sr (ppm)	Fe (ppm)	Mn (ppm)	$\delta^{13}C$ (‰) VPDB	$\delta^{18}O$ (‰) VPDB
Dahaneh-Kalut section									
Rd1	n	2						7	
	Avg.	54	46	117/5	73/5	10899	1692/5	0/30	−7/82
	Stdev,	1/414214	1/414214	27/57716	0/707107	9941/921	1277/742	0/392975	0/574545
	Max.	55	47	137	74	17929	2596	0/99	−6/99
	Min.	53	45	98	73	3869	789	−0/01	−8/45
Rd2	n	2						5	
	Avg.	52	48	120	48	6657	870/5	0/09	−8/98
	Stdev,	1/414214	1/414214	32/52691	11/31371	4690/946	357/0889	0/428553	0/383142
	Max.	53	49	143	56	9974	1123	0/73	−8/52
	Min.	51	47	97	40	3340	618	−0/36	−9/54
Rd3	n	5						8	
	Avg.	56	44	509/8333	83	16367/17	2941/5	0/51	−10/44
	Stdev,	2/19089	2/19089	147/3247	19/2873	4091/392	1374/434	0/428553	0/383142
	Max.	58	48	656	122	21990	4681	0/73	−8/52
	Min.	52	42	285	73	10702	1550	−0/36	−9/54
Cd	n	6						10	
	Avg.	57/33333	42/66667	495/5	103/3333	17560	3335/667	−0/48	−11/20
	Stdev,	0/816497	0/816497	162/2082	17/18914	4604/09	1810/437	0/656995	1/146395
	Max.	58	44	765	120	24221	5470	0/76	−9/87
	Min.	56	42	308	72	11832	1178	−1/66	−13/80
Ozbak-Kuh section									
Rd1	n	1						3	
	Avg.	53	47	114	75	1988	249	0/74	−6/22
	Stdev,	_	_	_	_	_	_	0/338291	0/154449
	Max.	_	_	_	_	_	_	0/98	−6/06
	Min.	_	_	_	_	_	_	0/35	−6/37
Rd2	n	6						9	
	Avg.	51/33333	48/66667	104	55/66667	5765/167	738/6667	0/48	−6/50
	Stdev,	0/516398	0/516398	38/78144	4/718757	1659/77	250/2252	0/716892	0/979402
	Max.	52	49	182	61	8731	998	1/47	−4/70
	Min.	51	48	79	49	3997	439	−0/36	−7/66

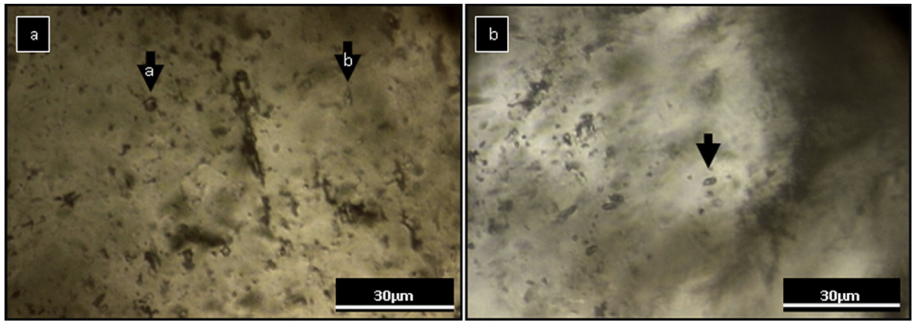

Fig. 10. Photomicrographs of fluid inclusions: a) irregular (arrow a) and elongate (arrow b) small fluid inclusions of saddle dolomite cement (Cd); and, b) small fluid inclusion in replacive dolomite (Rd3). The Gas-Phase represents ~25% of the total inclusion volume.

Table 2
Statistical summary of the fluid inclusions microthermometric results for the Rd3 and Cd dolomite types.

Dolomite types	T_h	T_m	Salinity
Rd3			
n	11		
Avg.	146.45		
Stdev,	14.67		
Max.	163		
Min.	122		
Cd (saddle dolomite)			
n	20		
Avg.	151.45	−20.43	21.308
Stdev,	12.86	5.56	2.35
Max.	175	−15	24
Min.	130	−27	18.63

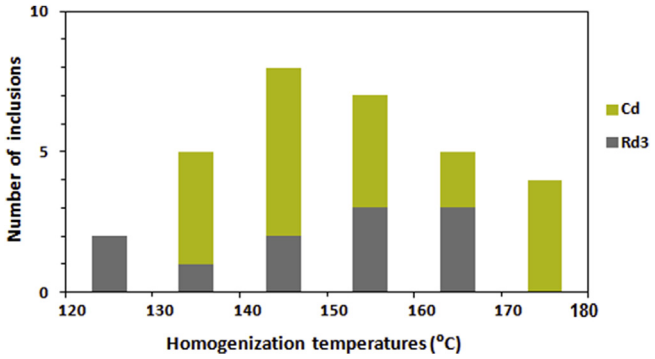

Fig. 11. Histogram of homogenization temperatures (°C) of fluid inclusions of Rd3 and Cd dolomite types. The homogenization temperature spans for Rd3 and Cd dolomite types vary within the same range and point to a similar origin for the fluids responsible for their formation.

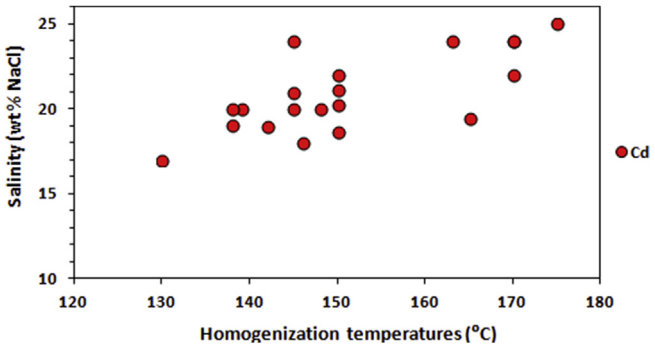

Fig. 12. Homogenization temperatures (°C) versus salinity (NaCl wt %) correlation diagram of fluid inclusions in Cd dolomite. These values were obtained from single fluid inclusion analysis and the temperature span is derived from the T_h original values from fluid inclusions without re-equilibration.

5.2. Constraints from isotope geochemistry and microthermometry

Stable isotope analyses of various dolomite types (Fig. 13 and Table 1) demonstrated that the $\delta^{18}O$ values in most types are depleted relative to the postulated values for Silurian marine carbonates (−2 to −6.5‰ VPDB; Azmy et al., 1998), while their $\delta^{13}C$ values show only low variations and differ from Silurian marine carbonates (−1 to 7.5‰ VPDB; Azmy et al., 1998). Plotting oxygen versus carbon stable isotopic values for the Niur Formation dolomite on an Allan and Wiggins (1993) diagram (Fig. 13) showed that, with some exceptions for the Ozbak-Kuh Rd1 and Rd2 dolomite types, most samples are located in the high temperature region. As mentioned earlier, the fine crystalline, planar textures and lack of evaporites suggest that Rd1 dolomite was possibly formed during an early stage of diagenesis at less than 50 °C temperatures from Silurian seawater (Gregg and Sibley, 1984). According to the paleotemperature equation of Friedman and O'Neil (1977), the expected $\delta^{18}O$ value for dolomite that precipitated from Silurian seawater (−3.5‰ SMOW, Azmy et al., 1998) at 20 °C during early stage diagenesis (Haeri-Ardakani et al., 2013a) is about 1.3‰ VPDB. However, the $\delta^{18}O$ values of Rd1 dolomite ranged from −6.06‰ to −6.37‰ VPDB at Ozbak-Kuh and −6.99‰ to −8.45‰ VPDB at Dahaneh-Kalut, which are more depleted than the estimated value (1.3‰ VPDB) for Silurian dolomite. This suggests that Rd1 was likely recrystallized under near-surface conditions with the incursion of meteoric water or at higher temperatures under burial conditions (Al-Aasm, 2000). Repeated recrystallization by meteoric water in near surface conditions before dolomitization is not supported by the near-micritic grain size and because the $\delta^{13}C$ values for Rd1 dolomite show comparable values to the postulated values for those of carbonates precipitated in equilibrium with Silurian seawater (−1 to 7.5‰). Also, field and petrographic evidence, such as lack of karst features and enhanced porosity do not support meteoric diagenesis. Although may cause depletion in the $\delta^{18}O$, petrographic investigations indicate that planar-e Rd1 dolomite replaces skeletal grains and likely lime-mud and calcite cements whereas planar-s Rd2 dolomite is pervasive. The isotope ratios for the latter dolomite overlap with Rd1 dolomite (Fig. 13). However, this overlap and the existence of Rd1 dolomite at the vicinity of Rd2 dolomite suggest that recrystallization of Rd1 dolomite likely happened during the formation of Rd2 dolomite, although it might also suggest that these dolomite types were precipitated from similar dolomitizing fluids at different temperatures (e.g., Lonnee and Machel, 2006; Azmy et al., 2008, 2009; Haeri-Ardakani et al., 2013b).

The occurrence of Rd3 dolomite and saddle dolomite cement (Cd) in the lower part of Dahaneh-Kalut in the vicinity of mafic volcanic rocks and fractures is possibly indicative of the role of fractures and volcanic activity in supplying the dolomitizing fluids (Lavoie and Morin, 2004). The coarse crystal size, non-planar texture, negative $\delta^{18}O$ values (Table 1) and the high homogenization temperatures of Rd3 dolomite and saddle dolomite cement (Cd) (Table 2; 146.4 °C ±14.6 °C and 151.4 °C ± 12.8 °C, respectively), support their late-stage precipitation at higher temperatures during burial and/or from hot basinal fluids (Radke and Mathis, 1980; Lonnee and Machel, 2006; Haeri-Ardakani et al., 2013a). The overlap in isotopic ratios and homogenization temperature values of Rd3 dolomite and saddle dolomite (Cd) can be related to either their formation at the same time or to replacement and/or recrystallization of Rd3 dolomite during late saddle dolomite formation (Al-Aasm, 2000). Although salinity measurements were not possible for Rd3 dolomite because of the small size (1–2 μm) of the fluid inclusions, the measured salinity for Cd (17–24 wt % NaCl eq.) indicates that it is was precipitated from highly saline fluids (e.g., Davies and Smith, 2006). To determine the $\delta^{18}O_{fluid}$ composition of Rd3 and Cd, their $\delta^{18}O$ values were plotted against their T_h counterparts (Fig. 14). In this plot, the calculated $\delta^{18}O_{fluid}$ for Rd3 dolomite ranges from +4 to +11‰ VSMOW and for Cd from +2 to +8‰ VSMOW. Mean values of T_h and $\delta^{18}O_{dolomite}$ VPDB of Rd3 and Cd fall near the boundary of the magmatic fluid field of composition. Such enriched values for the diagenetic fluids could be related to: 1) evaporation of marine waters (e.g., Hein et al., 1992; Haeri-Ardakani et al., 2013b), 2) water from evaporite dissolution, 3) some input of magmatic fluids ($\delta^{18}O$ VSMOW of +5.5 to +10‰; Taylor, 1979), 4) the effect of hydrothermal fluids (Spencer, 1987; Hou et al., 2016), or 5) combination of some or all of these factors (Lavoie and Chi, 2006). Since evaporated seawater at near gypsum

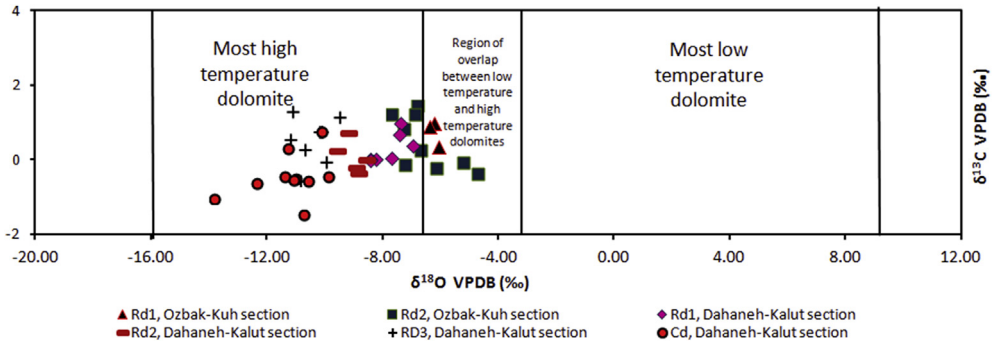

Fig. 13. Oxygen versus carbon stable isotope values for the Niur dolomite at the Ozbak-Kuh and Dahaneh-Kalut sections on an Allan and Wiggins (1993) diagram.

saturation would be 3 ± 1‰ enriched in $\delta^{18}O$ relative to contemporaneous sea-water (Gonfiantini, 1986), then the evaporated Silurian seawater (−3.5‰ SMOW) would have range $\delta^{18}O$ from −2.5 to −0.5‰ SMOW. Hence, evaporated Silurian seawater couldn't have supplied the dolomitizing fluids for theRd3 and Cd dolomite types. The lack of evaporated brine indicators, such as sulphate nodules and also the existence of normal marine fauna argue against brine origin. Devonian seawater with $\delta^{18}O$ −1‰ SMOW (Joachimski et al., 2009) could be considered ^{18}O-enriched relative to Silurian seawater. Accordingly, fluids that are supplied by dissolution of Devonian evaporites could have produced saline fluids with more positive $\delta^{18}O$ values. On the other hand, there are strong similarities and overlap between the obtained $\delta^{18}O_{fluid}$ values (Fig. 14) and the estimated values for magmatic fluids (+5.5 to +10‰ VSMOW, Taylor, 1979). These results suggest that fluids with other sources (such as dissolution of Devonian evaporates) could have been involved in supplying the dolomitizing fluids for the Rd3 and Cd, and possibly magmatic fluids or might have some contributions.

5.3. Major and trace elements constraints

Major and trace element concentrations in dolomite are controlled by the precursor carbonate mineral, the chemistry of dolomitizing fluids (Table 3), and the nature of the diagenetic environment (Fu et al., 2006; Kırmacı, 2008, 2013; Zhao and Jones, 2012; Azomani et al., 2013; Hou et al., 2016). The $CaCO_3$ and $MgCO_3$ concentrations of Rd1 dolomite (Table 1) revealed that it is non-stoichiometric. The Sr concentrations of this dolomite (73–75 ppm) are comparable to those of other ancient dolomite and are lower than the estimated values for dolomite in equilibrium with sea water (~500–800 ppm; e.g., Land, 1980). Rd2 dolomite is near stoichiometric and has lower Sr concentration values (average: 54 ppm) than Rd1 dolomite (average: 74 ppm). Thus the low Sr contents of Rd1 and Rd2 may argue against origin from rather than fluids with high salinity such as found in hypersaline sabkhas (<550 ppm; Tucker and Wright, 1990). The higher Sr concentrations of Rd3 and Cd (73–122 ppm) suggest that they precipitated from different fluids such as basinal brines (e.g., Sperber et al., 1984; Humphrey, 1988; Azmy et al., 2001, 2008; Azomani et al., 2013; Hou et al., 2016).

The average content of Na in the Rd1 and Rd2 dolomite types (110 ± 25 ppm) is comparable to the Na content of dolomite types that precipitate from normal seawater (about 110–160 ppm); this similarity may indicate that they were deposited from solutions of marine origin (Veizer, 1983; Qing and Mountjoy, 1988). Higher concentrations of Na in the Rd3 and Cd suggest that they were precipitated from more saline fluids with a different origin (Kırmacı, 2008, 2013; Azomani et al., 2013).

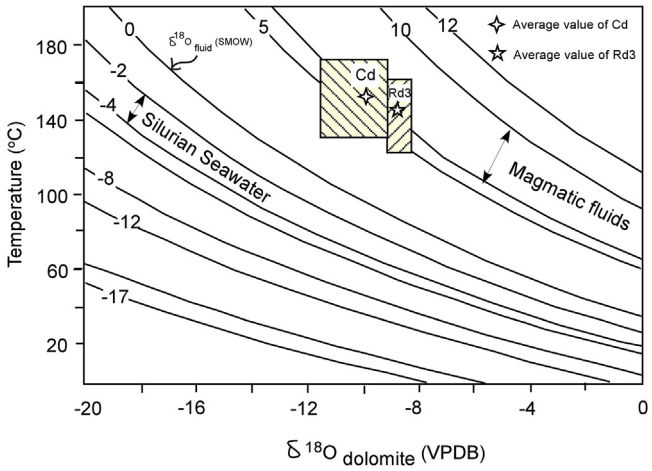

Fig. 14. Precipitation temperatures (°C) for the Rd3 and Cd dolomite types based on their T_h vs. $\delta^{18}O_{dolomite}$ (VPDB) values. $\delta^{18}O_{fluid}$ (SMOW) indicated by the values for the curves. Equilibrium lines derived from the fractionation equation: $10^3 \ln\alpha_{dolomite\text{-}water} = 3.2 \times 10^6 T^{-2} - 3.3$ (Land, 1985). $\delta^{18}O_{fluid}$ values for the magmatic fluids from Taylor (1979) and Silurian marine water is from Azmy et al. (1998). Boxes show range of homogenization temperatures and $\delta^{18}O_{dolomite}$ values of the Rd3 and Cd and the stars show their mean values.

Fe and Mn concentrations in dolomite reflect both the redox conditions and the concentration of these elements in the dolomitizing fluids (Budd, 1997). Fe and Mn concentrations in marine dolomite vary from 3 to 50 ppm (Veizer, 1983), although different values have also been reported (Vahrenkamp and Swart, 1990; Budd, 1997). The Fe and Mn concentrations in the Rd1 and Rd2 dolomite types are greater than those of dolomite precipitating from hot, saline, basinal fluids (Veizer, 1983; Aharon et al., 1987; Fouke, 1994). Very high Fe and Mn concentrations in the Rd3 and Cd dolomite reflect origin from entirely different diagenetic fluids than those of Rd1 and Rd2 dolomite types (e.g., Kırmaci, 2013; Hou et al., 2016). In general, the concentrations of Fe and Mn increase and $\delta^{18}O$ values decrease from RD1 to Cd (Fig. 15). The dramatically high Fe contents may suggest possible contribution from fluids associated with magmatic activities (e.g., Hou et al., 2016) or circulated through volcanic rocks.

6. Early Silurian magmatic activities and hydrothermal dolomitization

Field, petrographic observations and geochemical analyses suggest that the fluids that formed the Rd1 and Rd2 dolomite types were from a fluid that had contributions from seawater, likely mixed marine and meteoric waters that was formed during early to

Table 3
Trace element concentrations in seawater and magmatic fluids.

Trace elements	Seawater (Veizer, 1983)	Magmatic fluids (Yang and Scott, 2006)
Sr (ppb)	8	3505–23,657
Na (ppm)	10,760	9595–17,106
Mn (ppb)	0.2	13,725–195,389 × 1000
Fe (ppb)	2	1786–872,165 × 1000

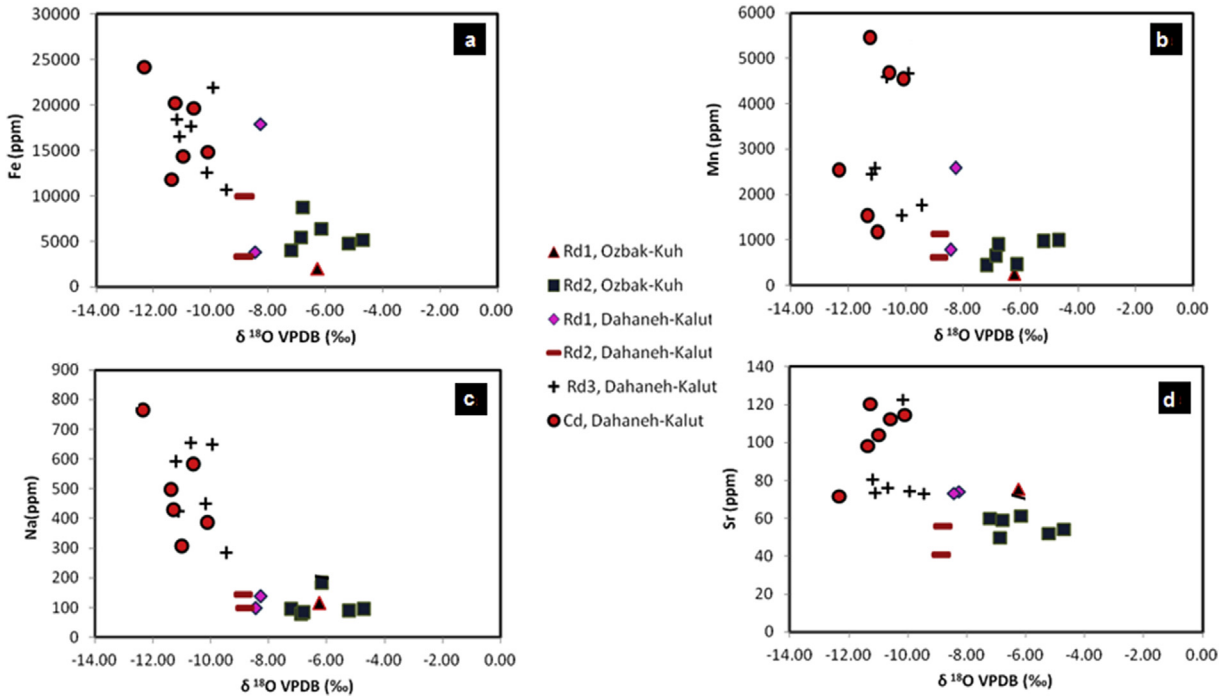

Fig. 15. Cross plots of $\delta^{18}O$ versus the Fe, Mn, Na and Sr concentrations of the different dolomite types in the Dahaneh-Kalut and Ozbak-Kuh sections. Negative trends can be related to the increase of magmatic fluid activity of the dolomitizing fluids during progressive burial dolomitization.

intermediate stages of burial respectively. In contrast, Rd3 and Cd, which are present only in the lower and middle parts of the Dahaneh-Kalut, are related to fractures and volcanic activity.

Fracture-related dolomite usually forms during tectonic activity (Davies and Smith, 2006). Hence, we can infer that the Rd3 and Cd dolomite types formed during the early Silurian to the Devonian during a time of major tectonic activity (Berberian and King, 1981; Lasemi, 2001). Petrographic, stable isotopes and micro-thermometric analyses also demonstratet hat the Rd3 and Cd precipitated from hot fluids with a medium to high salinity either during burial (Machel and Lonnee, 2002). Due to the lack of burial history data for the Niur Formation, it is difficult to conclude that the Rd3 and Cd dolomite types are possibly hydrothermal. In order to shed light on this problem, petrographic and geochemical data were used from dolomite in the underlying the Ordovician Shirgesht Formation and from the overlying Devonian Padeha Formation (Zand-e-Moghadam, 2013) in the Dahaneh-Kalut section. The data demonstrate that dolomitization is the final burial diagenetic phase in the Shirgesht carbonate rocks and the two dolomite types (d1 and d2) are present in this formation. The size of the crystals of the d1 and d2 dolomite types are similar to those of Rd1 and Rd2, ranging from 10 to 20 μm and 20–50 μm, respectively (Fig. 16). Oxygen isotope values (Table 4) of the d1 and d2, as the final burial diagenetic phase of the Shirgesht Formation, are heavier than found in the final burial dolomitization phase (Rd3 and Cd) of the Niur Formation. Additionally, the latest dolomitization phase of the Padeha dolomite gives maximum formation temperatures about 80–85 °C (Zand-e-Moghadam, 2013). These temperatures are lower than those calculated temperatures for the latest dolomite phase of the Niur Formation (Nowrouzi, 2015). The oxygen isotopic values for the Ordovician Shirgesht dolomite (−7.4 to −6.52‰ VPDB) and the lower T_h values for the Padeha dolomite (80–85 °C) showed that the Niur Formation was not deeply buried during Silurian to Devonian time. These results a long with the presence of corroded and broken Rd3 and Cd dolomite crystals that are cut by stylolites as well as Rd3 dolomite clasts breccia that are filled by early Cd dolomite, suggest that these dolomite types were formed at shallow to intermediate burial depths (e.g., Davies and Smith, 2006) by much hotter fluids, likely hydrothermal (e.g., Machel, 2004). The Rd3 and Cd dolomite types have similarities with hydrothermal dolomite reported in the literature with respect to salinity, homogenization temperatures and $\delta^{18}O_{fluids}$ SMOW values (Davies and Smith, 2006).

Submarine mafic volcanic rocks at the base of the Niur Formation are attributed to the initial stages of intracontinental passive rifting in late Ordovician to early Silurian times in central Iran (Berberian and King, 1981; Stampfli et al., 1991; Lasemi, 2001; Aghanabati, 2004). These volcanic rocks, which are related to extensional tectonics during an early Silurian rifting phase, were responsible for the flow of fluids that were likely much hotter than the surrounding environment and of hydrothermal origin. The presence of mafic volcanic rocks directly below and above the Rd3 and Cd created a local thermal gradient that led to circulation of fluids through voids and fractures, thereby affecting the

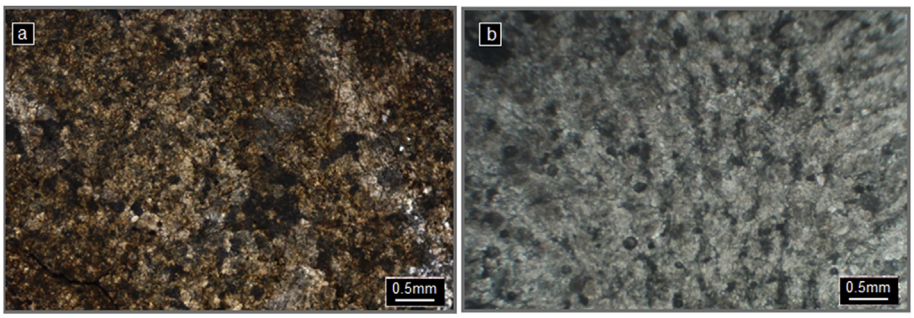

Fig. 16. Photomicrographs of the Shirgesht dolomite (XPl): a) fine crystalline dolomite (d1); and b) medium crystalline dolomite.

Table 4
Carbon and oxygen isotope ratios of dolomite the Shirghesht Formation at the Dahaneh-Kalut section.

Samples No.	Dolomite types	$\delta^{13}C$ VPDB (‰)	$\delta^{18}O$ VPDB (‰)
S3	Rd1	0.04	−6.52
S4	Rd1	−0.01	−6.68
S5	Rd2	−0.34	−7.03
S7	Rd2	−0.25	−7.4

surrounding carbonate rocks. This resulted in the Cd dolomite to be precipitated within voids and fractures and the Rd3 dolomite replacing the surrounding carbonate rocks. The lower values of $\delta^{18}O$ in the Rd1 and Rd2 dolomite of the Dahaneh- Kalut section, relative to those at Ozbak-Kuh, are also indicative of a local thermal gradient and/or higher burial temperatures at Dahaneh- Kalut than at Ozbak-Kuh.

7. Fluids flow models and the potential source(s) of Mg^{+2} for hydrothermal dolomitization

Since extensional magmatic activities are usually accompanied by elevated heat flows (Davies and Smith, 2006), we propose a possible thermal convection circulation model for the formation of Dahaneh-Kalut hydrothermal dolomite (Evans and Nunn, 1989; Coniglio et al., 1994; Yao and Demicco, 1995, 1997; Morrow, 1998; Demicco and Spencer, 2004; Morrow and Aulstead, 2004). In this model (Fig. 17), Mg-rich fluids could have been recycled many times through the precursor carbonates and generated massive pervasive dolomite (Morrow, 1998; Wilson et al., 2001). Microthermometry and geochemical analyses suggest that fluids responsible for the formation of Rd3 and Cd dolomite types relatively much hotter than Rd1 and Rd2. The more abundant the Rd3 and Cd dolomite types at the base of the Dahaneh-Kalut section suggest that their dolomitizing fluids originated at the base of the Niur Formation.

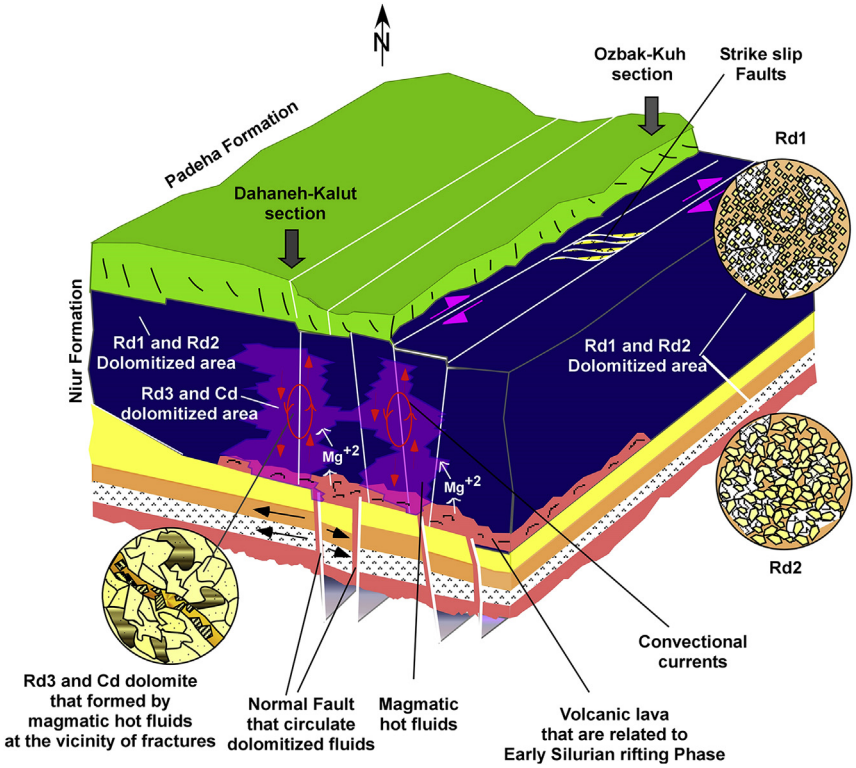

Fig. 17. Dolomitizing model for the Niur Formation in the Dahaneh-Kalut and Ozbak-Kuh sections. Note that the Rd3 and Cd dolomite types are only present in the Dahaneh-Kalut section, and Rd1 and Rd2 dolomite types occur in both sections. This model shows the effect of the tectonic setting and magmatic activity on both heat and fluid flows in the formation.

Mafic volcanic rocks at the base of the Dahaneh-Kalut section supplied Mg for hydrothermal dolomitization similar to that proposed for the hydrothermal dolomitization patterns found in the Lower Silurian dolomite in eastern Canada (Lavoie and Chi, 2006) and the Upper Carboniferous dolomite of Spain (Gasparrini et al., 2006). According to this model a late Ordovician to early Silurian passive rifting phase led to the generation of a local thermal gradient and elevated heat flows that circulated Mg- bearing fluids with a magmatic origin among the precursor carbonate rocks. During this process, a network of fractures associated with rifting faults provided open conduits that focused the hydrothermal fluid ~~s~~ flow and the generation of the Rd3 and Cd dolomite types in the vicinity (Rd3) and in the fractures (Cd). It is also possible that the magmatic associated fluids contributed to the basinal dolomitizing fluids that already existed and the mixed fluids flew mainly through fractures that precipitated Rd3 and Cd dolomite types.

8. Conclusions

Carbonate rocks of the Silurian Niur Formation of east Central Iran were pervasively dolomitized. Integrated Petrographic, geochemical and fluid inclusion analyses from two different stratigraphic sections suggest the presence of four different types of dolomite that are categorized as replacive (Rd1 to Rd3) and saddle dolomite cement (Cd). The investigation results suggest that:

1) Rd1 and Rd2 dolomite types formed during early and intermediate stages of diagenesis. The Rd3 and Cd dolomite, which occlude fractures observed only at Dahaneh-Kalut, occur in the vicinity of mafic volcanic rocks and close to the base of the Niur Formation.
2) Low values of $\delta^{18}O$ (Rd3 = −9.47‰ to −11.21‰VPDB, Cd = −9.87‰ to −13.80‰VPDB) and high T_h values of Rd3 (122° to 163 °C) and Cd (130° to 175 °C), respectively, as well as being cross-cut by stylolites, suggest that hydrothermal fluids of possible magmatic origin were involved in for the formation of these dolomite types. This is also consistent with the similarities and overlaps between the $\delta^{18}O_{magmatic\ fluids}$ values and the estimated values of the parent dolomitizing fluids.
3) Major and trace element analyses show that the Rd3 and Cd compositions are very distinct from those of Rd1 and Rd2, thus suggesting origin from different parent fluids. The enrichment in Fe contents of Rd3 and Cd supports contributions from magmatic-activity related fluids
4) Petrographic and geochemical comparison of the Ordovician Shirgesht and Devonian Padeha dolomite with the Niur dolomite show that the Niur Formation was not deeply buried during dolomitization.
5) The similarities between petrography and geochemistry of Rd3 and Cd and those of hydrothermal dolomite types and the extensional tectonic setting of Niur Formation suggest a hydrothermal dolomitization model for the formation the Rd3 and Cd.
6) This model suggests that magmatic activities are related to a late Ordovician to early Silurian rifting phase that generated a local thermal gradient with an increase in heat flow and caused thermal convectional fluids to circulate and supply dolomitizing fluids for the Rd3 and Cd dolomite types. Other supporting evidence, such as the formations of Rd3 and Cd in the vicinity of mafic rocks and fractures, also support this hypothesis.
7) This study has shown that the roles of tectonic setting and thermal conditions are important for the generation and circulation of dolomitizing fluids as well as for the formation of large scale massive dolomite.

Acknowledgments

The authors would like to acknowledge the Ferdowsi University of Mashhad, Iran for financial supports and field works. This manuscript is part of the PhD thesis by Z. Nowrouzi at Ferdowsi University of Mashhad and also researches by A. Mahboubi during sabbatical leave in the Department of Earth and Environmental Sciences, University of Windsor, Canada. We would like to acknowledge Drs. Graham Davies, David Symons and Omid Haeri-Ardakani and also anonymous reviewers for their suggestions and comments that improve our manuscript significantly. ISA would like to acknowledge NSERC (812005) for its support.

References

Aghanabati, A., 2004. Geology of Iran. Geological Survey of Iran (In Persian), p. 586.
Aharon, P., Socki, R.A., Chan, L., 1987. Dolomitization of atolls by sea water convection flow: test of a hypothesis at Niue, South Pacific. J. Geol. 95, 187–204.
Al-Aasm, I.S., 2000. Chemical and isotopic constraints for recrystallization of sedimentary dolomites from the Western Canada sedimentary basin. Aquat. Geochem. 6, 229–250.
Al-Aasm, I.S., Ghazban, F., Ranjbaran, M., 2009. Dolomitization and related fluid evolution in the Oligocene – Miocene Asmari Formation, Gachsaran area, SW Iran: petrographic and isotopic evidence. J. Pet. Geol. 32 (3), 287–304.
Alavi, M., 1996. Tectonostratigraphic synthesis and structural style of the Alborz Mountainous system in Northern Iran. J. Geodyn. 11, 1–33.
Allan, J.R., Wiggins, W.D., 1993. Dolomite Reservoirs. Geo-chemical Techniques for Evaluating Origin and Distribution. In: AAPG Continuing Education Course Notes Series, vol. 36, p. 129.
Azmy, K., Veizer, J., Bassett, M.G., Copper, P., 1998. Oxygen and carbon isotopic composition of Silurian brachiopods: implications for coeval seawater and glaciations. Geol. Soc. Am. Bull. 110 (11), 1499–1512.
Azmy, K., Veizer, J., Misi, A., De Olivia, T., Dardenne, M., 2001. Isotope stratigraphy of the neoproterozoic carbonate of Vazante Formation, Saõ Francisco Basin Brazil. Precambrian Res. 112, 303–329.
Azmy, K., Lavoie, D., Knight, I., Chi, G., 2008. Dolomitization of the Aguathuna Formation carbonates of Port au Port Peninsula in western Newfoundland, Canada: implications for a hydrocarbon reservoir. Can. J. Earth Sci. 45, 795–813.
Azmy, K., Knight, I., Lavoie, D., Chi, G., 2009. Origin of the Boat Harbour dolomites of St. George Group in western Newfoundland, Canada: implications for porosity controls. Bull. Can. Pet. Geol. 57, 81–104.
Azomani, E., Azmy, K., Blamey, N., Brand, U., Al-Aasm, I.S., 2013. Origin of Lower Ordovician dolomites in eastern Laurentia: controls on porosity and implications from geochemistry. Mar. Pet. Geol. 40, 99–114.
Berberian, M., King, G.C., 1981. Towards the paleogeography and tectonic evolution of Iran. Can. J. Earth Sci. 18, 210–265.
Bodnar, R.J., 2003. Interpretation of data from aqueous-electrolyte fluid inclusions. In: Samson, I., Anderson, A., Marshal, D. (Eds.), Fluid Inclusions: Analyses andInterpretation. Short Course Series, vol. 32. Mineralogical Association of Canada, pp. 81–100.
Budd, D.A., 1997. Cenozoic dolomites of carbonate islands: their attributes and origin. Earth Sci. Rev. 42, 1–47.
Chen, D., Qing, H., Yang, C., 2004. Multistage hydrothermal dolomites in the Middle Devonian (Givetian) carbonates from the Guilin area, South China. Sedimentology 51, 1029–1051.
Coniglio, M., Sherlock, R., Williams-Jones, A.E., Middleton, K., Frape, K., 1994. Burial and hydrothermal diagenesis of Ordovician carbonates from the Michigan Basin, Ontario, Canada. In: Purser, B., Tucker, M., Zenger, D. (Eds.), Dolomites: International Association of Sedimentologists Special Publication, vol. 21, pp. 231–254.
Davies, G.R., Smith, L.B., 2006. Structurally controlled hydrothermal dolomite reservoir facies: an overview. Am. Assoc. Pet. Geol. Bull. 90 (11), 1641–1690.
Demicco, R.V., Spencer, R.J., 2004. Constraints on dolomitization from models of brine origin and flow modeling. In: McAuley, R. (Ed.), Dolomites — the Spectrum: Mechanisms, Models, Reservoir Development. Canadian Society of Petroleum Geologists, Seminar and Core Conference, January 13-15, Calgary.
Dickson, J., 1965. A modified staining technique for carbonates in thin section. Nature 205, 587.
Evans, D.G., Nunn, J.A., 1989. Free thermohaline convection in sediments surrounding a salt column. J. Geophys. Res. 94 (12), 412–422.
Flügel, H.W., 1962. Korallen aus dem Silur von Ozbak-Kuh (NE-Iran). Jahrb. Geol. Bundesanst. 105, 287–330.
Flügel, H.W., Saleh, H., 1970. Die paläozoischen Korallen faunen Ost-Irans. 1. Rugose Korallen der Niur Formation (Silur). Jahrb. Geol. Bundesanst. 113, 267–302.
Fouke, B.W., 1994. Deposition, Diagenesis, and Dolomitization of Neogene Seroedomi Formation Coral Reef Limestones on Curacao, Netherlands Antilles (Natuur wetenschappelijke Studiekringvoor het Caraibisch Gebied (Publications Foundation for Scientific Research in the Caribbean Region), 133), p. 182 (Amsterdam).
Friedman, I., O'Neil, J.R., 1977. Compilation of stable isotopes fractionation factors of

geochemical interest. In: Feischer, M. (Ed.), Data of Geochemistry, p. 12. US Geological Survey Professional Paper, 440.
Fu, Q., Qing, H., Bergman, K.M., 2006. Dolomitization of the Middle Devonian Winnipegosis carbonates in south-central Saskatchewan, Canada. Sedimentology 53, 825–848.
Goldstein, R.H., Reynolds, T.J., 1994. Systematics of Fluid Inclusions in Diagenetic Minerals. Society for Sedimentary Geology (SEPM) Short Course, Tulsa, Okla.
Gonfiantini, R., 1986. Environmental isotopes in lake studies. In: Fritz, P., Fontes, J.C. (Eds.), Handbook of Environmental Isotope Geochemistry, vol. 113, p. 68.
Gasparrini, M., Bechstädt, T., Boni, M., 2006. Massive hydrothermal dolomites in the southwestern Cantabrian Zone (Spain) and their relation to the Late Variscan evolution. Mar. Pet. Geol. 23, 543–568.
Gregg, J.M., Sibley, D.F., 1984. Epigenetic dolomitization and the origin of xenotopic dolomite texture. J. Sediment. Pet. 54, 908–931.
Haeri-Ardakani, O., Al-Aasm, I.S., Coniglio, M., 2013a. Fracture mineralization and fluid flow evolution: an example from Ordovician–Devonian carbonates, southwestern Ontario, Canada. Geofluids 13, 1–20.
Haeri-Ardakani, O., Al-Aasm, I.S., Coniglio, M., 2013b. Petrologic and geochemical attributes of fracture-related dolomitization in Ordovician carbonates and their spatial distribution in southwestern Ontario, Canada. Mar. Pet. Geol. 43, 409–422.
Hairapetian, V., Blom, H., Miller, C.G., 2008. Silurian thelodonts from the Niur Formation, central Iran. Acta Palaeontol. Pol. 53, 85–95.
Hairapetian, V., Mohibullah, M., Tilley, L.J., Williams, M., Miller, C.G., Afzal, J., Ghobadi-Pour, M., Hejazi, S.M., 2011. Early Silurian carbonate platform ostracods from Iran: a peri-Gondwanan fauna with strong Laurentian affinities. Gondwana Res. 20, 645–653.
Hall, D.L., Sterner, S.M., Bodnar, R.J., 1988. Freezing point depression of NaCl-KCl-HZ0 solutions. Econ. Geol. 83, 197–202.
Hein, J.R., Gray, S.C., Richmond, B.M., White, L.D., 1992. Dolomitization of quaternary reef limestone, Aitutaki, Cook Islands. Sedimentology 39 (4), 645–661.
Hou, Y., Azmy, K., Berra, F., Jadoul, F., Blamey, N.J.F., Gleeson, S.A., Brand, U., 2016. Origin of the Breno and Esino dolomites in the western southern Alps (Italy): implications. Mar. Pet. Geol. 69, 38–52.
Humphrey, J.D., 1988. Late Pleistocene mixing zone dolomitization, southeastern Barbados, West Indies. Sedimentology 35, 327–348.
Joachimski, M.M., Breisig, S., Buggisch, W., Talent, J.A., Mawson, R., Gereke, M., Morrow, J.M., Day, J., Weddige, K., 2009. Devonian climate and reef evolution: insights from oxygen isotopes in apatite. Earth Planet. Sci. Lett. 284, 599–609.
Jacquemyn, C., El-Desouky, H., Hunt, D., Casini, G., Swennen, R., 2014. Dolomitization of the Latemar platform: fluid flow and dolomite evolution. Mar. Pet. Geol. 55, 43–67.
Kırmacı, M.Z., 2008. Dolomitization of the late Cretaceouse Paleocene platform carbonates, Gölköy (Ordu), eastern Pontides, NE Turkey. Sediment. Geol. 20, 289–306.
Kırmacı, M.Z., 2013. Origin of dolomite in the Late Jurassic platform carbonates, Bolkar Mountains, central Taurides, Turkey: petrographic and geochemical evidence. Chem. Erde – Geochem. 73 (3), 383–398.
Land, L.S., 1980. The isotopic and trace element geochemistry of dolomite: the state of the art. In Concepts and Models of Dolomitization. In: Zenger, D.H., Dunham, J.B., Ethington, R.L. (Eds.), Society of Economic Paleontologists and Mineralogists, Special Publication, 28, pp. 87–110.
Land, L.S., 1985. The origin of massive dolomite. J. Geol. Educ. 33, 112–125.
Lasemi, Y., 2001. Facies Analysis, Depositional Environments and Sequence Stratigraphy of the Upper Pre-cambrian and Paleozoic Rocks of Iran. Iran Geological Survey Publications, 180 (In Persian).
Lavoie, D., Morin, C., 2004. Hydrothermal dolomitization in the Lower Silurian Sayabec Formation in northern Gaspé-Matapé dia (Que bec): constraint on timing of porosity and regional significance for hydrocarbon reservoirs. Bull. Can. Pet. Geol. 52 (3), 256–271.
Lavoie, D., Chi, G., 2006. Hydrothermal dolomitization in the Lower Silurian La Vieille Formation in northern New Brunswick: geological context and significance for hydrocarbon exploration. Bull. Can. Pet. Geol. 54 (4), 380–395.
Lavoie, D., Chi, G., 2010. Lower Paleozoic foreland basins in eastern Canada: tectonothermal events recorded by faults, fluids and hydrothermal dolomites. Bull. Can. Pet. Geol. 58 (1), 17–35.
Lavoie, D., Chi, G., Urbatsch, M., Davis, W.J., 2010. Massive dolomitization of a pinnacle reef in the Lower Devonian West Point Formation (Gaspé Peninsula, Quebec): an extreme case of hydrothermal dolomitization through fault-focused circulation of magmatic fluids. Am. Assoc. Pet. Geol. Bull. 94 (4), 513–531.
Lonnee, J., Machel, H.G., 2006. Pervasive dolomitization with subsequent hydrothermal alteration in the Clarke Lake gas field, middle Devonian Slave Point formation, British Columbia, Canada. AAPG Bull. 90 (11), 1739–1761.
Machel, H.G., Lonnee, J., 2002. Hydrothermal dolomite — A product of poor definition and imagination. Sediment. Geol. 152, 163–171.
Machel, H.G., 2004. Concepts and models of dolomitization: a critical reappraisal. In: Braithwaite, C.J.R., Rizzi, G., Darke, G. (Eds.), The Geometry and Petrogenesis of Dolomite Hydrocarbon Reservoirs, Geological Society of London Special Publication 235, pp. 7–63.
Mazzullo, S., 1992. Geochemical and neomorphic alteration of dolomite: a review. Carbonates Evaporites 7, 21–37.
Morrow, D.W., 1998. Regional subsurface dolomitization: models and constraints. Geosci. Can. 25 (2), 57–70.
Morrow, D.W., Aulstead, K.L., 2004. Convection-driven sub-surface hydrothermal dolomitization in Middle Devonian-age shallow water limestones in the 0.4 tcf Kotaneelee gas field of southeastern Yukon territory. In: McAuley, R. (Ed.), Dolomites — the Spectrum: Mechanisms, Models, Reservoir Development: Canadian Society of Petroleum Geologists, Seminar and Core Conference, January 13 – 15, 2004, Calgary (Extended Abstracts, CD format).
Nader, F.H., Swennen, R., Ellam, R., 2004. Reflux Stratabound Dolostone and Hydrothermal Volcanism-associated Dolostone: a Two-stage Dolomitization Model (Jurassic, Lebanon), vol. 51, pp. 339–360.
Nadimi, A., 2007. Evolution of the central Iranian basement. Gondwana Res. 12, 324–333.
Nowrouzi, Z., Mussavi- Harami, R., Mahboubi, A., Mahmudy Gharaie, M.H., Ghaemi, F., 2014. Petrography and geochemistry of Silurian Niur sandstones, Derenjal Mountains, East Central Iran: implications for tectonic setting, provenance and weathering. Arabian J. Geosci. 7, 2793–2813.
Nowrouzi, Z., 2015. Facies Analysis, Depositional Environment and Geochemistry of Silurian Niur Formation in the Central Iran. PhD thesis. Ferdowsi University of Mashhad, Iran, p. 256.
Olanipekun, B.J., Azmy, K., Brand, U., 2014. Dolomites of the Boat Harbour Formation in the Northern Peninsula, western Newfoundland, Canada:Implications for dolomitization history and porosity control. Am. Assoc. Pet. Geol. Bull. 98 (4), 765–791.
Qing, H., Mountjoy, E.W., 1988. Multistage dolomitization in Rainbow Buildups, Middle Devonian Keg River Formation, Alberta, Canada. J. Sediment. Petrol. 59, 114–126.
Radke, B.M., Mathis, R.L., 1980. On the formation and occurrence of saddle dolomite. J. Sediment. Petrol. 50 (4), 1149–1168.
Ruttner, A.W., Nabavi, M.H., Hajian, J., 1968. Geological survey of Iran, Reports. Geology of the Shirgesht area (Tabas area, east Iran), vol. 4, pp. 1–133.
Roedder, E., 1984. Fluid inclusions, mineralogical society of America. Rev. Mineral. 12, 644.
Sengör, A.M.C., 1987. Tectonics of the Tethysides: orogenic collage development in a collisional setting. Annu. Rev. Earth Planet Sci. 15, 213–244.
Sibley, D.F., Gregg, J.M., 1987. Classification of dolomite rock texture. J. Sediment. Petrol. 57, 967–975.
Sperber, C.M., Wilkinson, B.H., Peacor, D.R., 1984. Rock composition, dolomite stoichiometry, and rock/water reactions in dolomitic carbonate rocks. J. Geol. 92 (6), 609–622.
Spencer, R.J., 1987. Origin of Ca – Cl brines in Devonian formations, Western Canada sedimentary basin. Appl. Geochem. 2, 373–384.
Stampfli, G., Marcoux, J., Baud, A., 1991. Tethyan margins in space and time. Palaeogeogr. Palaeoclimatol. Paleoecol. 87, 373–409.
Tucker, M.E., Wright, V.P., 1990. Carbonate Sedimentology. Blackwell, Oxford, p. 482.
Taylor Jr., H.P., 1979. Oxygen and hydrogen isotope relations in hydrothermal mineral deposits. In: Barnes, H.L. (Ed.), Geochemistry of Hydrothermal Ore Deposits. Wiley, New York, pp. 236–277.
Vahrenkamp, V.C., Swart, P.K., 1990. New distribution coefficient for the incorporation of strontium into dolomite and its implications for the formation of ancient dolomites. Geology 18, 387–391.
Veizer, J., 1983. Chemical Diagenesis of Carbonates: Theory and Application of Trace Element Technique. In: Stable Isotopes in Sedimentary Geology. Society of Economic Paleontologists and Mineralogists short course, 10, 3–100. Tulsa.
Warren, J., 2000. Dolomite: occurrence, evolution and economically important associations. Earth Sci. Rev. 52, 1–81.
Wilson, A.M., Sanford, W.E., Whitaker, F.A., Smart, P.L., 2001. Spatial patterns of diagenesis during geothermal circulation in carbonate platforms. Am. J. Sci. 301, 727–752.
Yang, K., Scott, S.D., 2006. Magmatic fluids as a source of metals in seafloor hydrothermal systems. Back-arc spreading systems: geological, biological, chemical, and physical interactions. Geophys. Monogr. 166, 163–184.
Yao, Q., Demicco, R.V., 1995. Paleoflow patterns of dolomitizing fluids and paleohydrogeology of the southern Cana-dian Rocky Mountains: evidence from dolomite geometry and numerical modeling. Geology 23 (9), 791–794.
Yao, Q., Demicco, R.V., 1997. Dolomitization of the Cambrian carbonate platform, southern Canadian Rocky Mountains: dolomite front geometry, fluid inclusion geochemistry, isotopic signature and hydrogeologic modelling studies. Am. J. Sci. 297, 892–938.
Zhao, H., Jones, B., 2012. Genesis of fabric-destructive dolostones: a case study of the Brac Formation (Oligocene), Cayman Brac, British West Indies. Sediment. Geol. 267-268, 36–54.
Zand-e-Moghadam, H., 2013. Facies Analysis, Provenance, Geochemistry, Diagenesis and Sequence Stratigraphy of Padeha Formation in the Central Iran. PhD thesis. Ferdowsi University of Mashhad, Iran, p. 380.